# Fluctuations in the diffuse X-ray background observed with *Ginga*

J. A. Butcher,[1] G. C. Stewart,[1] R. S. Warwick,[1] A. C. Fabian,[2] F. J. Carrera,[3] X. Barcons,[3] K. Hayashida,[4,5] H. Inoue[4] and T. Kii[4]

[1]*Department of Physics and Astronomy, Leicester University, University Road, Leicester, LE1 7RH*
[2]*Institute of Astronomy, Madingley Road, Cambridge CB3 0HA*
[3]*Instituto de Física de Cantabria (Consejo Superior de Investigaciones Científicas, Universidad de Cantabria), 39005 Santander, Spain*
[4]*Institute of Space and Astronautical Science, 3-1-1 Yoshinodai, Sagamihara, Kanagawa 229, Japan*
[5]*Department of Earth and Space Science, Osaka University, Machikaneyama, Toyonaka, Osaka 560, Japan*

**ABSTRACT**
We present *Ginga* measurements of the spatial fluctuations in the diffuse X-ray background. When combined with earlier results, the new data constrain the extragalactic $\log N$–$\log S$ relation in the 2–10 keV energy band to a form close to the Euclidean prediction over the flux range $10^{-10}$–$5 \times 10^{-13}$ erg cm$^{-2}$ s$^{-1}$. The normalization of the 2–10 keV source counts is a factor 2–3 above that derived in the softer 0.3–0.5 keV band from the *Einstein* Extended Medium Sensitivity Survey, if a spectral conversion is assumed which ignores X-ray absorption intrinsic to the sources. Both this result and the spectral characteristics of the spatial fluctuations are consistent with relatively low-luminosity active galaxies (i.e. $L_X < 10^{44}$ erg s$^{-1}$) dominating the 2–10 keV source counts at intermediate flux levels. We also use the 'excess variance' of the fluctuations to constrain possible clustering of the underlying discrete sources.

**Key words:** galaxies: active – diffuse radiation – X-rays: general.

## 1 INTRODUCTION

Since the discovery of the diffuse X-ray background (XRB) there has been considerable debate as to whether its origin lies solely in the integrated emission of known types of extragalactic X-ray source, such as Seyfert galaxies and QSOs, or whether a significant contribution might come from a hitherto undiscovered population of discrete X-ray sources. The alternative, that much of the XRB might originate in diffuse emission from a putative intergalactic medium, has been effectively rejected through measurements of the microwave background spectrum using the *COBE* satellite (Mather et al. 1990; Barcons, Fabian & Rees 1991).

In modelling the XRB in terms of discrete sources a continual frustration is the fact that the surface brightness and spectral form of the XRB are well determined only above 3 keV, whereas the most detailed studies of the source populations have been carried out in the soft X-ray band (through the exploitation of the imaging systems on *Einstein*, *EXOSAT* and *ROSAT*). In the 2–10 keV band, which contains a significant fraction of the XRB energy density, our knowledge of the X-ray luminosity and spectra of individual sources is restricted mainly to the relatively bright sources which appear in the all-sky catalogues of *Uhuru*, *Ariel 5* and *HEAO-1*. However, the statistical properties of sources at much fainter fluxes are accessible through studies of spatial fluctuations in the XRB.

Radio astronomers were the first to recognize that, by studying the beam-to-beam variations in the sky background in directions away from bright catalogued sources, it was possible to derive information on sources too faint to be resolved individually. The theoretical basis for such fluctuation studies is well documented (Scheuer 1974; Condon 1974). Provided source clustering effects can be neglected (see Barcons 1992), the form of the background fluctuations distribution, the so-called $P(D)$ distribution, is governed solely by the $\log N$–$\log S$ relation of the discrete sources which produce the fluctuations and by the normalized beam response of the detector. It can be shown that, for simple power-law forms of $N(S)$, the shape of the $P(D)$ distribution depends on $\gamma$, whereas the width of the $P(D)$ distribution scales as $(K\Omega_e)^{1/\gamma-1}$, where $\Omega_e$ is the effective beamsize (see Condon 1974). We use the differential form of the $\log N$–

log $S$ relation, in which the number of sources per steradian, in the flux range from $S$ to $S + dS$, is given by

$$N(S)\,dS = KS^{-\gamma}\,dS.$$

Here $K$ is the normalization of the differential source counts and $\gamma$ the power-law slope; note that $\gamma = 2.5$ corresponds to the Euclidean form of the source counts.

The standard analysis approach is one of model-fitting, in which a predicted $P(D)$ curve is computed and compared to the observed distribution. The properties of the underlying log $N$–log $S$ relation can then be inferred through the process of minimizing the differences between the predicted and observed fluctuation distributions. Although the spatial fluctuations are the result of the combined influence of sources over a very wide flux range, in practice most information is extracted at flux levels corresponding to a surface density of about 1 source per beam (Scheuer 1974). It follows that the narrower the detector beam, the fainter the flux level reached. An important proviso is, of course, that the fluctuations must be measured with an adequate signal-to-noise ratio for useful information to be obtained.

In the present paper we show that measurements of spatial fluctuations by *Ginga* provide constraints on the 2–10 keV source counts and source clustering at flux levels corresponding to a surface density of extragalactic X-ray sources of $\sim 1$ object per square degree. Similar levels are encompassed in the *Einstein* Observatory Extended Medium Sensitivity Survey (EMSS) (Gioia et al. 1990b), and a comparison is made between the source count estimates in the medium energy and soft X-ray regimes (i.e. the 2–10 keV and 0.3–3.5 keV bands). We also comment on the spectral characteristics of the spatial fluctuations measured by *Ginga*.

There have been several previous studies of XRB fluctuations as measured in the medium energy X-ray band (e.g. Fabian 1975; Schwartz, Murray & Gursky 1976; Pye & Warwick 1979; Shafer 1983). Of these, the most definitive result is from the *HEAO-1* A2 survey in which the XRB data were derived from detectors with collimated fields-of-view of $3° \times 3°$ and $3° \times 1.5°$ (Shafer 1983). Here we present measurements of spatial fluctuations in the XRB made with the Large Area Counter (LAC) on *Ginga*. Since the collimated beam of the LAC is only $1° \times 2°$, the *Ginga* measurements are potentially more sensitive than those from *HEAO-1* A2. Full details of the LAC, which had a total effective area of $\sim 4000$ cm$^2$, several times larger than that of the *HEAO-1* A2 experiment, are given in Turner et al. (1989). Preliminary results from this study have been reported by Warwick & Stewart (1989), Hayashida (1990) and Warwick & Butcher (1992). *Ginga* observations (the same data as used here) have also been used to study the angular autocorrelation function of the X-ray background (Carrera et al. 1991).

The paper is organized as follows: Section 2 presents the estimates of source counts based on the analysis of the *Ginga* fluctuations. Upper limits to the excess variance required in the fitting procedure are used to constrain source clustering. The spectrum of the fluctuations is also analysed. Section 3 is devoted to the discussion of these results, and in particular to the comparison of the inferred source counts with the EMSS. Section 4 summarizes our results.

## 2  THE *GINGA* MEASUREMENTS

### 2.1  The observations

The data used in the fluctuation analysis come from two types of observation: dedicated raster scans of the background and observations taken as part of the normal background monitoring programme. In total, the data set comprises 132 independent pointings. The data were all taken in MPC1 mode (Turner et al. 1989) and we use only data from the top layer of the LAC (separation of data from the top and mid-layers of the LAC gives an improved signal-to-noise ratio for weak sources). In all of the observations the angle between the LAC pointing direction and the sun was greater than 90°, thus excluding any possibility of contamination of the data by solar X-rays.

Since *Ginga* had no facility for simultaneous background measurement during a source observation, a typical *Ginga* observation consisted of one day pointing at the source followed by a further day pointing at a nearby region of 'blank' sky. Over the lifetime of the mission there thus accumulated a large data base of potentially useful background observations. Here we utilize 70 such observations of independent sky regions made between 1987 June and 1989 August. We selected only observations with $|b| > 25°$. Where there existed multiple pointings in the same direction we chose the one with the largest exposure. The typical exposure of an observation is $\sim 20\,000$ s. Fig. 1 shows the distribution of these observations over the sky. It should be noted that the distribution of these pointings is neither uniform nor random but follows, to first order, the distribution of X-ray sources above the *Ginga* limiting sensitivity.

The second source of data is from three sets of dedicated background observations performed in 1988 January, 1988 July and 1989 March. In each case a set of independent regions of sky were observed at the rate of one region per satellite orbit, giving a typical exposure time per pointing of $\sim 1500$ s. The three areas of sky observed in this way were situated near the north and south Galactic poles and the north ecliptic pole.

### 2.2  Extraction of the background fluctuations

The LAC registered counts from charged particles and other events as well as from cosmic X-rays. Both the count rate and the spectrum of the LAC internal background varied with time in a complex manner (see Hayashida et al. 1989). Over a period of $\sim 24$ hr, most of the variation of the background could be explained by the change in cut-off rigidity with satellite altitude and by radioactive decays induced by the passage of the satellite close to the South Atlantic Anomaly (SAA). In addition, a 37-d periodicity was present as a result of the precession of the satellite orbit, which caused the height of the daily passage through the SAA to vary. There was also a very long-term decrease in the background which was related to the gradual decay of the satellite orbit. The internal background of the LAC was modelled using a development of the methods described in Hayashida et al. (1989), although the exact method employed was slightly different for the two different types of data.
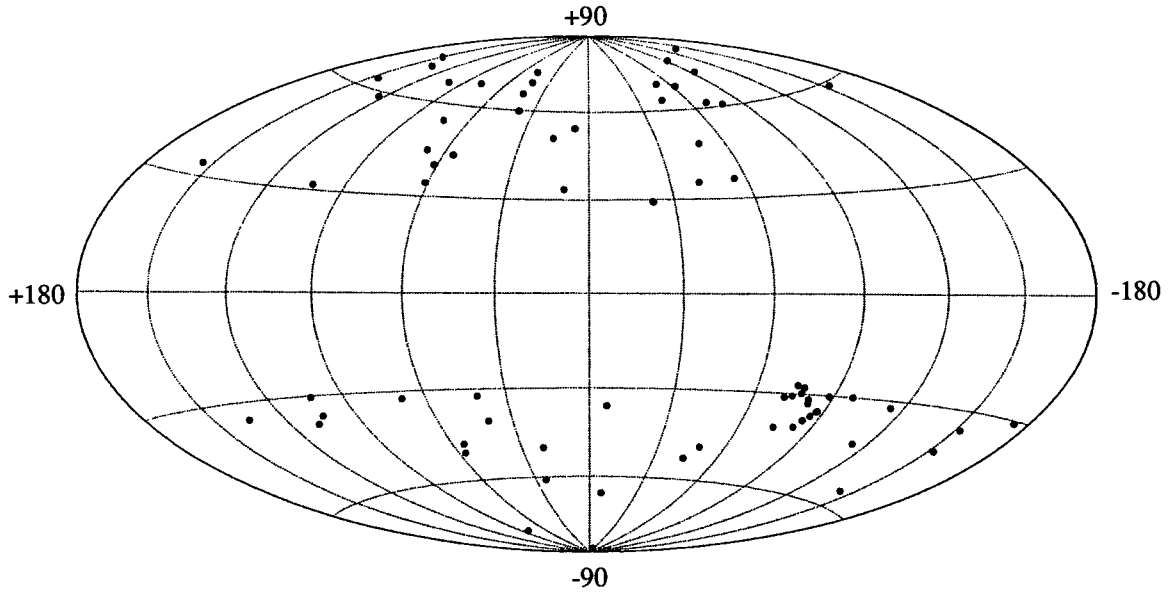
**Figure 1.** The distribution of background observations obtained from the *Ginga* data base shown in galactic coordinates. The concentration in the bottom right-hand corner corresponds to background observations made during the regular monitoring of SN 1987A.

Each set of dedicated observations lasted only 1–2 d, so the long-term variations could be ignored. For each data set we fitted a time series model of the form

$$I(E, t) = a_1(E) + \sum_{i=2}^{6} a_i(E) \times x_i(t),$$

where $I(E, t)$ is the LAC count rate as a function of energy channel and time, $x_i(t)$ are five time-dependent parameters derived from LAC housekeeping data and $a_i(E)$ are scaling coefficients which represent the spectral forms of the corresponding background components. More specifically, two of the $a_i$ coefficients represent contributions which scale with the SUD (counts Surplus to Upper Discriminator) and with the cut-off rigidity, whereas the other three represent the spectra of induced radioactive decays with empirically-derived e-folding times of 12.5, 1 and 0.5 h. The time-independent term $a_1(E)$ is the average over the data set of the cosmic diffuse background plus any residual particle background in the detector. The best-fitting values of $a_1$ and the five $a_i$ coefficients for each set of dedicated observations were used to create a background model for that data set. The deflection or fluctuation level was then determined for each individual pointing direction as the difference between the observed count rate and the modelled value.

The equivalent procedure for the observations drawn from the *Ginga* data base was slightly more complicated. As the observations were spread over a longer time period it was necessary to model the variations in internal background caused by the 37-d precession of the satellite orbit (Hayashida et al. 1989). Ideally, such modelling requires many observations spread over all phases of the 37-d period. There was also the problem of the long-term drift of the internal background induced by the decay of the satellite orbit. The latter proved difficult to incorporate directly in the fitting procedure and, as a first approach to minimizing any long-term drift whilst attempting to optimize the model-

ling of the 37-d component, the 70 observations were simply divided into two data sets containing 36 and 34 pointings, each of which spanned roughly 13 months. A background model of the form discussed earlier was then applied to each of these data sets, except that the $a_i$ coefficients modelling the induced radioactivity incorporated a (best-fitting) 37-d variation. The fluctuation level for a particular observation was again determined as the difference between the observed count rate and that derived from the background model for the data set. Finally a check was made for evidence of any obvious trends in the time-ordered fluctuation measurements from each data set; however, no significant long-term effects were apparent, thus validating the analysis procedure.

## 2.3 Analysis of the $P(D)$ distributions

The $P(D)$ distributions measured by *Ginga* in two energy ranges (2–4 and 4–12 keV) are shown in Fig. 2. The rms widths of the distributions correspond to approximately $\sim 0.4$ count s$^{-1}$, which corresponds to roughly 5 per cent of the predicted count rate from the XRB in the two bands (using predictions based on the XRB spectrum reported by Marshall et al. 1980).

We fit the observed $P(D)$ curves using trial source count distributions of power-law form via standard Fourier transform techniques based on the method of Condon (1974). Full account is taken of the beam profile of the LAC collimators. The $\log N$–$\log S$ relationship is truncated when the integrated intensity exceeds the total background strength, although (as explained earlier) the shape of the $P(D)$ is not sensitive to fluxes where the $N(S)$ curve predicts many sources per beam. The effects of counting statistics and residual errors in the fitting procedure described above are included by convolving the model $P(D)$ curve with a Gaussian of standard deviation $\sigma \approx 0.1$ count s$^{-1}$. This is the appropriate statistical error for the short $1$–$2 \times 10^3$ s scan
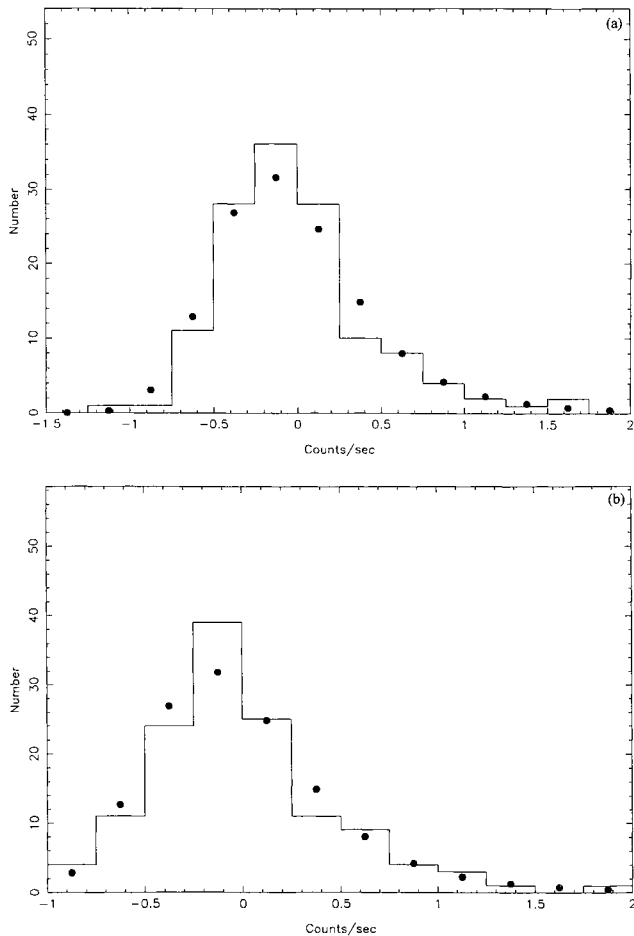
**Figure 2.** The measured $P(D)$ histograms in the (a) 2–4 keV band and (b) 4–12 keV band, together with the best-fitting model predictions (filled circles).

observations, while for the longer pointings the value is dominated by the systematic errors in the background modelling procedure. For the data base pointings, the value of $\sigma$ was estimated by comparing repeated observations of the same region of sky. The results are not sensitive to the exact value of $\sigma$ within appropriate limits. [We note that this is the first time that XRB fluctuation measurements have been made where the $P(D)$ noise is several times the statistical error on individual samples.]

### 2.4 Constraints on the log *N*–log *S* relation

The observed fluctuation distributions were fitted with model $P(D)$ curves, via a process of $\chi^2$ minimization. (The results thus obtained were entirely consistent with those produced by an alternative approach, namely the maximum likelihood method – see the next section). This fitting procedure led to the constraints on the power-law slope, $\gamma$, and normalization, $K$, of the log *N*–log *S* relation shown in Fig. 3. The parameters of the best-fitting models, for which the predicted $P(D)$ curves are shown in Fig. 2, are listed in Table 1, where the quoted errors correspond to 90 per cent confidence for one interesting parameter. Table 1 also gives the best-fitting normalizations for the $\gamma = 2.5$ case, that is a Euclidean slope for the source counts. Finally, Table 1 also
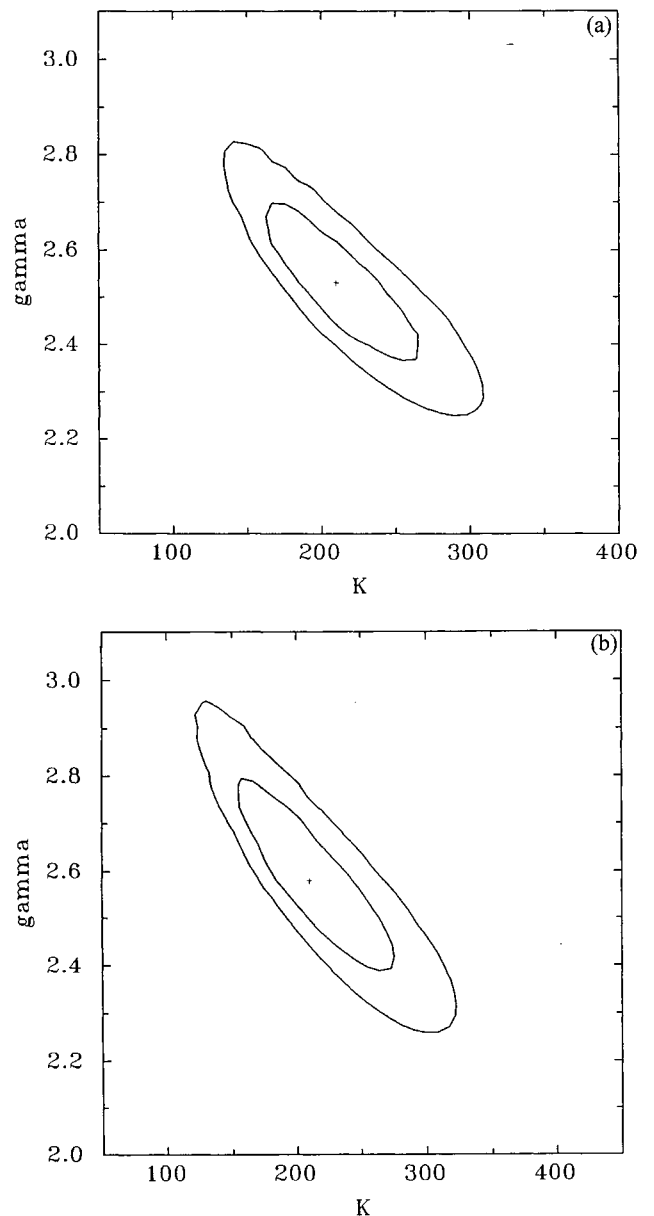


**Figure 3.** $1\sigma$ and 90 per cent contours in the $K$, $\gamma$ parameter space for (a) the 2–4 keV band and (b) the 4–12 keV band. $K$ is in units of $(\mathrm{LAC\ count\ s}^{-1})^{\gamma-1}\,\mathrm{sr}^{-1}$.

gives the normalizations converted to 2–10 keV flux units, using a conversion factor based on the response of *Ginga* to a power-law spectrum with an energy index of $\alpha = 0.8$ (we show later that this is an appropriate value for $\alpha$).

The best-fitting slopes for both energy ranges are consistent with each other and with the Euclidean value of $\gamma = 2.5$. The inferred Euclidean 2–10 keV source count normalizations in the two energy bands are also in excellent agreement with each other and with the normalization of the resolved-source counts reported by Piccinotti et al. (1982).

### 2.5 Excess variance

So far we have explicitly neglected source clustering in the computation of the model $P(D)$ distribution. It is customary

**Table 1.** The parameters of the best-fitting source-count models. The normalization values are quoted in both count rate and flux units.

| | 2–4 keV Band | | | 4-11 keV Band | | |
|---|---|---|---|---|---|---|
| | $\gamma$ | K $^a$ | K $^b$ | $\gamma$ | K $^a$ | K $^b$ |
| Overall best-fit | $2.53^{+0.15}_{-0.13}$ | $210^{+53}_{-36}$ | $0.88^{+0.20}_{-0.15}$ | $2.58^{+0.18}_{-0.14}$ | $210^{+60}_{-38}$ | $0.22^{+0.07}_{-0.04}$ |
| Euclidean case | 2.5 | $218^{+54}_{-36}$ | $2.0^{+0.5}_{-0.3}$ | 2.5 | $234^{+56}_{-41}$ | $2.0^{+0.5}_{-0.3}$ |

$^a$In units of $(LAC \ \text{count} \ s^{-1})^{\gamma-1} \ sr^{-1}$.
$^b$In units of $10^{-15} \ (\text{erg} \ cm^{-2} \ s^{-1})^{\gamma-1} \ sr^{-1}$.

(Fabian & Rees 1978; Shafer 1983) to mimic the effects of source clustering by convolving the predicted distribution of fluctuations for unclustered sources with a Gaussian of standard deviation $\sigma_{excess}$ and then to try to measure or constrain this parameter via a comparison with the observational data.

In order to study the allowed range for the excess variance, we have used a maximum likelihood method, since checks revealed that, in this case, binning the data and minimizing the $\chi^2$ function did appear to give systematically higher values (by up to 20 per cent) of $\sigma_{excess}$ than did the maximum likelihood approach. We have computed the likelihood function in $(K, \gamma, \sigma_{excess})$ parameter space. We then consider $K$ and $\gamma$ as non-interesting parameters and for all their values we select the maximum likelihood as a function of $\sigma_{excess}$ only. This function is then normalized to give a measure of probability.

We find that the value of $\sigma_{excess}$ that maximizes the likelihood function is less than 0.05 count s$^{-1}$, which is of the same order as the errors in the fluctuation measurements. Thus there is no clear evidence for effects arising from source clustering. At the $1\sigma$ level $\sigma_{excess} < 0.17$ count s$^{-1}$, and at $2\sigma$ confidence $\sigma_{excess} < 0.3$ count s$^{-1}$. In relative terms those upper limits correspond to $\Delta I/I < 2$ per cent and $\Delta I/I < 3.8$ per cent. It must be stressed that the $2\sigma$ upper limit corresponds to a situation in which there is a very low surface density source population, and most of the width of the $P(D)$ curve comes from the excess variance. These results

on source clustering are entirely consistent with the results of Carrera et al. (1991), who use the same data reported here to calculate the autocorrelation function of the X-ray background and obtain only upper limits.

The $2\sigma$ upper limit $\Delta I/I < 3.8$ per cent imposes some interesting cosmological constraints. In terms of Poisson fluctuations this limit implies a minimum of 345 sources deg$^{-2}$, whereas Shafer (1983) obtained a limit of 2 per cent for a 25 deg$^2$ beam, thus requiring a minimum of only 100 sources deg$^{-2}$. The present measurements impose stringent constraints on any large-scale inhomogeneities of the X-ray universe (see Fabian & Barcons 1992). This is emphasized in Fig. 4, where the upper bounds to $\delta\rho/\rho$ (assuming that X-rays trace mass on large scales) implied by the lack of significant excess variances are shown. It is assumed that the sources that dominate the fluctuations in the LAC are concentrated at a mean redshift of about $z = 0.5$ with a spread $\Delta z = 0.5$, which is very roughly consistent with the EMSS redshift distribution. The present data provide the best direct evidence for the linearity of the fluctuations in the Universe on scales greater than several tens of Mpc at those early redshifts.

### 2.6 The spectrum of the fluctuations

A further potentially valuable source of information on source properties at relatively faint flux levels is provided by the spectral characteristics of the spatial fluctuations in the XRB. We have extracted the spectral form of the fluctuations by subtracting the average spectrum of 'negative' fluctuations from that of 'positive' fluctuations. (The spectral parameters are very mildly dependent on the definition of 'negative' and 'positive' fluctuations).

The resulting spectrum was then analysed by a standard model-fitting procedure. We assume a power-law spectral form and initially fit the data over the 2–11 keV range. The fit was formally acceptable and the derived spectral parameters were $\alpha = 0.82^{+0.04}_{-0.03}$ and $N_H < 0.9 \times 10^{21}$ cm$^{-2}$ (errors are $1\sigma$ for two interesting parameters). Since the fluctuations are dominated by sources with a surface density of roughly one per beam, this reflects the average spectrum of sources producing about 10 per cent of the 2–10 keV XRB. It is notable that the fluctuation spectrum has a power-law slope which is typical of Seyfert 1 galaxies in the 2–10 keV band. Of interest, however, is an extrapolation of the best-fitting spectrum to higher energies. This reveals an apparent hardening of the spectrum above 10 keV. Indeed, the simple spectral model described above did not yield a statistically acceptable fit over the 2–18 keV band ($\chi^2/\nu = 39.5/24$). In this case the derived spectral parameters were $\alpha = 0.80^{+0.03}_{-0.04}$
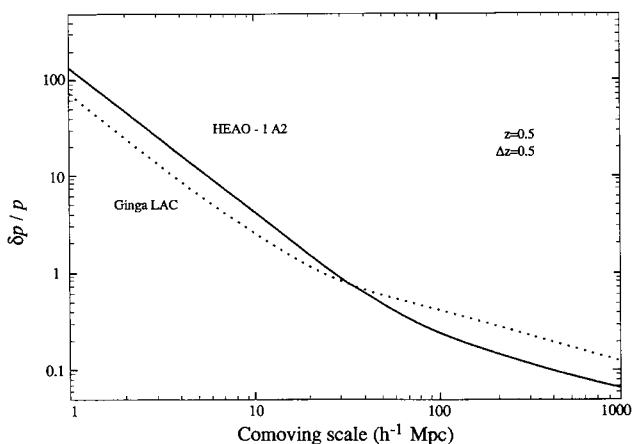


**Figure 4.** Upper bounds to inhomogeneities as a function of comoving scale based on the $2\sigma$ upper limits to the excess fluctuations from *HEAO-1* A2 and *Ginga*. It is assumed that fluctuations come from a redshift range $\Delta z = 0.5$ around $z = 0.5$.
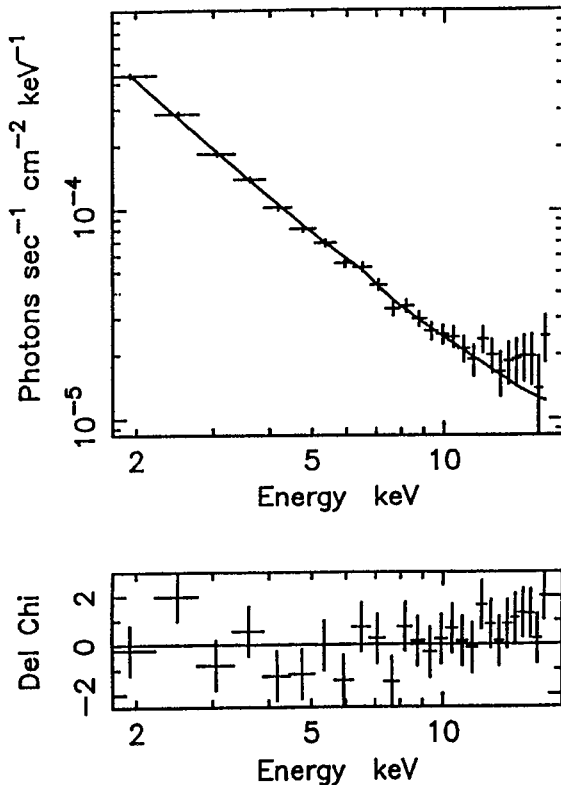
and $N_H < 0.5 \times 10^{21}$ cm$^{-2}$ but, in view of the bad fit, clearly these should be treated with caution.

The apparent 'hard excess' is reminiscent of the features apparent in spectra of Seyfert 1 galaxies, which have been attributed to a Compton reflection bump (e.g. Pounds et al. 1990). In fact, the inclusion of a Compton reflection component in the current analysis results in a significant improvement in the 2–18 keV spectral fit ($\chi^2/\nu = 26.7/24.3$). In this case the spectral parameters were $\alpha = 0.90^{+0.10}_{-0.07}$, $N_H < 1.5 \times 10^{21}$ cm$^{-2}$ with the fraction of reprocessed flux being $\sim 50$ per cent. Fig. 5 shows the measured spectrum of the fluctuations and the best-fitting model.

# 3   DISCUSSION

## 3.1   The 2–10 keV X-ray source counts

The 2–10 keV source counts for bright ($S > 3 \times 10^{-11}$ erg cm$^{-2}$ s$^{-1}$) extragalactic sources have been determined from the *Ariel 5*, *Uhuru* and *HEAO-1* A2 all-sky surveys (Warwick & Pye 1978; Schwartz 1979; Piccinotti et al. 1982). There is good agreement between the three surveys on the normalization of the source counts, which is hardly surprising given the fact that the small 'statistical samples' derived from each survey (typically $\sim 60$ sources in each case) overlap to a considerable extent. The derived slope of the bright source counts is marginally steeper than the Euclidean value, but this appears to be the result of the chance distribution of a few nearby sources rather than being of direct cosmological significance (Piccinotti et al. 1982). At fainter levels we must

rely on spatial fluctuation measurements. This is illustrated in Fig. 6 which shows the form of the 2–10 keV differential source counts derived from the Piccinotti discrete source sample and from both the *HEAO-1* A2 (Shafer 1983) and present *Ginga* fluctuation measurements.

The *HEAO-1* A2 fluctuation measurements best define the source counts at flux levels about a factor of 6 below the threshold of the Piccinotti sample, whereas the new *Ginga* results provide additional constraints at flux levels *a factor of 30 below* the Piccinotti limit, a flux which will only be directly probed by imaging medium energy telescopes.
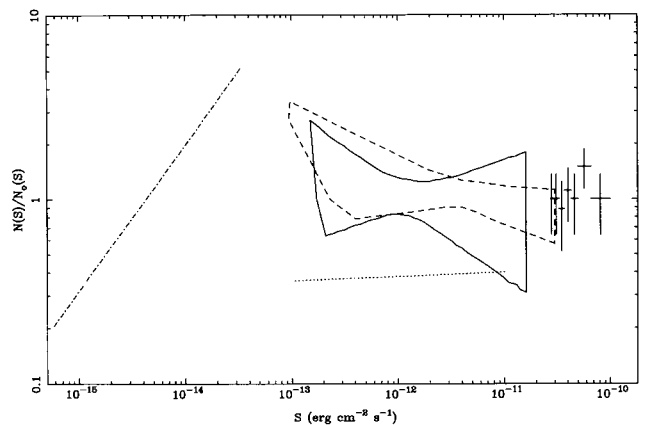
The discrete source and spatial fluctuation data taken together constrain the $\log N$–$\log S$ relation to a form close to the Euclidean prediction over almost three decades of flux. Specifically, the 2–10 keV differential counts are consistent with

$$N(S)\,dS = 2 \times 10^{-15}\, S^{-2.5}\, dS\ \mathrm{sr}^{-1}$$

over the range $S = 10^{-10}$–$5 \times 10^{-13}$ erg cm$^{-2}$ s$^{-1}$ (2–10 keV).

We note that, although the fluctuation measurements include a contribution from Galactic sources (which are, of course, specifically excluded from the discrete source sample), the net effect of Galactic sources, particularly at the lower flux levels, will be small ($\lesssim 10$ per cent contribution to $K$ at $S = 10^{-12}$ erg cm$^{-2}$ s$^{-1}$). Similarly, the effect of possible large-scale structure in the XRB, for example due to Galactic diffuse emission and the Compton–Getting anisotropy, is unlikely to introduce a significant bias (Shafer 1983; Carrera et al. 1991). As we noted earlier, source clustering might contribute to an overestimate of the source counts, but it would have to be implausibly strong to seriously affect our conclusions (Carrera et al. 1993).

The fact that the extragalactic source counts have a slope close to the Euclidean value necessarily implies some cosmological evolution of the source population, since the effects of relativistic geometry will be quite pronounced

**Figure 5.** The spectrum of the fluctuations (top panel) and the residuals (bottom panel) after fitting a model including a reflection component.

**Figure 6.** The differential source counts in the 2–10 keV band normalized to $N_0(S) = 2 \times 10^{-15} S^{-2.5}$. Points are from Piccinotti et al. (1982), the dashed contour is the 90 per cent contour from *HEAO-1* A2 fluctuations (Shafer 1983) and the solid curve is the 90 per cent contour from the present fluctuation analysis. The dotted line shows the EMSS prediction assuming $f = 1$ (see text). The dash-dotted line to the left represents the boundary of the region where a particular power-law extrapolation completely produces the XRB.

© 1997 RAS, MNRAS **291**, 437–445

even for the modest redshifts which correspond to source luminosities typically in the range $L_X = 10^{42-45}$ erg s$^{-1}$.

## 3.2 Comparison with soft X-ray source counts

The *Ginga* fluctuation studies extend the 2–10 keV source counts to flux levels encompassed in the 0.3–3.5 keV band by the EMSS (Gioia et al. 1990b) and it is clearly of interest to compare the $\log N$–$\log S$ relations derived in the two spectral regimes.

In principle such a comparison requires knowledge of the spectral properties of the contributing source populations over a wide energy range (0.3–10 keV). However, a convenient simplification (e.g. Boldt 1988) is to define an average spectral conversion factor $f$ as

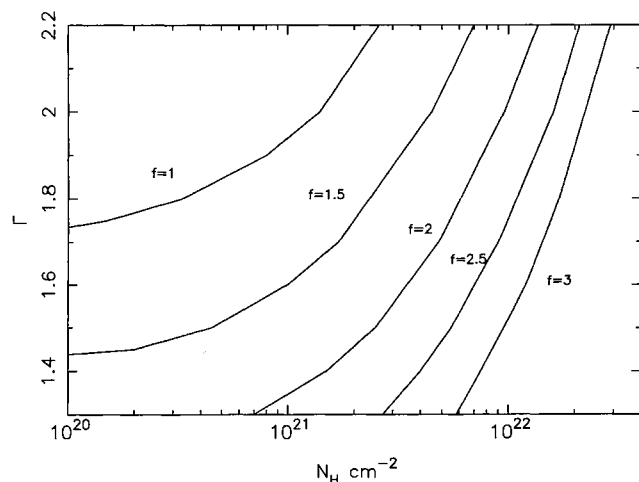$$f = \frac{S_{2-10}}{S_{0.3-3.5}},$$

where $S_{2-10}$ is the flux measured in the 2–10 keV band and $S_{0.3-3.5}$ is the corresponding value in the 0.3–3.5 keV band.

If a particular value of $f$ applies to the whole source population, then the differential source count normalizations in the two bands are related by

$$K_{2-10} = f^{\gamma-1} \times K_{0.3-0.5}.$$

For a source with a power-law spectrum of spectral energy index $\alpha = 0.7$ [the so-called canonical spectral slope for active galactic nuclei (AGN)] and negligible low-energy absorption (we actually assume a minimum line-of-sight column density of $N_H = 3 \times 10^{20}$ cm$^{-2}$), then $f \sim 1$. Fig. 7 shows the effect on $f$ of varying the power-law slope and intrinsic absorption. Using $f = 1$, the extragalactic $\log N$–$\log S$ relation from the EMSS (Gioia et al. 1990b) transforms to the dotted line in Fig. 6. Clearly the above assumptions lead to the conclusion that our fluctuation analysis produces a significant (i.e., a factor of 2–3) overestimation of the soft X-ray source counts, as measured by the *Einstein* Observatory.

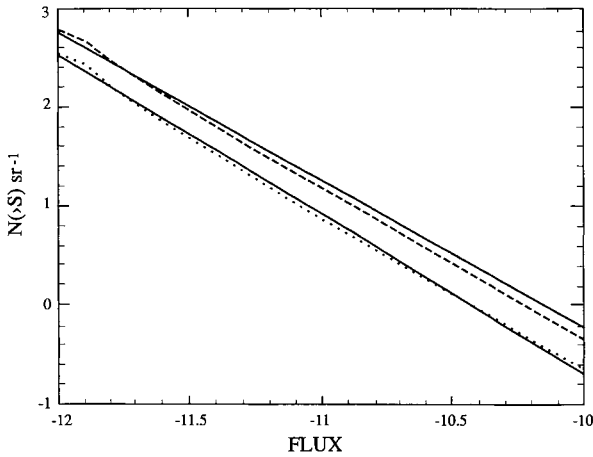To reconcile the EMSS and 2–10 keV source counts requires $f \sim 2.0$ for the source population as a whole. This implies either a continuum spectrum which is significantly less steep than the canonical form (i.e., $\alpha \sim 0.4$) or a spectrum which is cut-off at low energies, presumably due to X-ray absorption in relatively cold line-of-sight gas intrinsic to the source. For the canonical spectral slope, $f \sim 2.0$ implies $N_H \sim 3 \times 10^{21}$ cm$^{-2}$. This is barely consistent with the upper limit for photoelectric absorption found in the spectrum of the fluctuations (but see below). Nevertheless, given the available information on the spectra of extragalactic X-ray sources (e.g. Maccacaro et al. 1988), a solution in terms of absorption would seem to be the more tenable.

The EMSS results (Gioia et al. 1990b; Stocke et al. 1991) confirm that AGN, namely Seyfert galaxies and QSOs, comprise the dominant source population at intermediate flux levels with other classes of source (clusters of galaxies, normal galaxies and BL Lac objects) providing up to a 25 per cent contribution to the extragalactic source counts. Since it is well established that low-luminosity AGN preferentially exhibit intrinsic absorption (e.g. Reichert et al. 1985; Turner & Pounds 1989), it would seem reasonable to infer that it is this class of source which is under-represented in the EMSS. The presence of such a spectral selection effect may well account for at least part of the flattening in the luminosity function of AGN below $L_X \sim 10^{43}$ erg s$^{-1}$ reported in the EMSS sample (Maccacaro et al. 1991). Observations of individual Seyfert I galaxies suggest that intrinsic absorption is common in sources with luminosities less than about $3 \times 10^{43}$ erg s$^{-1}$ (Turner & Pounds 1989). Also, it is well known that the more numerous Seyfert 2 galaxies show strong absorption. Absorption by a column density of $\sim 10^{22}$ cm$^{-2}$ will strongly suppress the emission in the soft band of the EMSS (0.3–3.5 keV) but will have little effect on the 4–12 keV band of *Ginga*.

In order to test the above hypothesis, we have constructed simple model X-ray source counts. We calculated the cluster contribution taking into account the cluster luminosity function of Edge et al. (1990), the negative evolution shown by the clusters (Edge et al. 1990; Gioia et al. 1990a) and the observed temperature luminosity relation (Edge & Stewart 1991). The residual source counts were then compared to the model predictions for AGN. We used the AGN luminosity function of Piccinotti et al. (1982) and assumed luminosity evolution of the form $(1+z)^C$ (see e.g. Maccacaro et al. 1991; Boyle et al. 1993). An energy index of 0.7 is assumed. Intrinsic absorption corresponding to a column density of $N_H = 10^{22} N_{22}$ cm$^{-2}$ is applied to all the AGN with luminosities below $L^{abs}$. An important parameter is the assumed minimum luminosity of the AGN population, $L_{min}$, which controls the total contribution of AGN to the X-ray background. In practice we expect there to be a break to a flatter luminosity function, but here we simply truncate the luminosity function at $L_{min}$.

After searching parameter space we find that $C \sim 2.5$, $N_{22} \sim 1$, $L_{min} \sim 3 \times 10^{42}$ erg s$^{-1}$ and $L_{abs} \sim 10^{43}$ erg s$^{-1}$ give total (AGN plus cluster) source counts which agree with Piccinotti et al. (1982), the source counts derived from the $P(D)$ found here and the EMSS counts (see Fig. 8). The summed spectrum of the sources brighter than $S = 10^{-12}$ erg cm$^{-2}$ s$^{-1}$ is shown in Fig. 9. It is seen that it is well-fitted over the 3–12 keV band by a power law with $\alpha = 0.76$, the softer spectra of the clusters having steepened the total spectrum slightly. It is in reasonable agreement



**Figure 7.** Curves of constant $f$ for values of photon spectral index, $\Gamma$, and absorbing column, $N_H$, typical of AGN.

**Figure 8.** The integrated source counts from the AGN model described in the text. The upper solid line represents the fiducial model in the 2–10 keV band after subtracting the cluster contribution. The lower solid line corresponds to the EMSS measurement. The dashed and dotted lines correspond to the integrated counts from AGN in the hard and soft bands respectively. The flux units are $\log(S_{2-10})$ for the hard source counts and $\log(S_{0.5-3.5})$ for the soft counts.
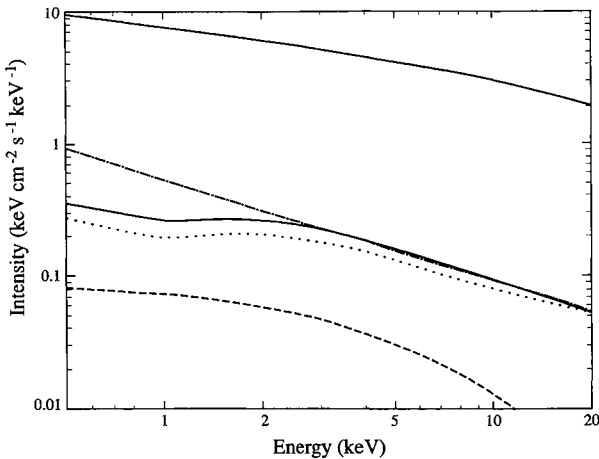
**Figure 9.** The cumulative contribution (lower solid line) of AGN (dotted line) and clusters (dashed line) brighter than a 2–10 keV flux of $S = 10^{-12}$ erg cm$^{-2}$ s$^{-1}$ is compared with the intensity of the XRB obtained from Gruber's (1992) formula (upper solid curve). The best-fitting power-law in the range 3–12 keV to the AGN contribution is shown by the dash-dotted line. It has an energy index of 0.76, slightly steeper than that of the underlying AGN spectra of index 0.70.

with the observed 2–10 keV spectral fluctuations. Significant deviations from a power law are only clear below 3 keV, where the absorption from the low-luminosity AGN becomes effective. The total AGN contribution at 4 keV, extrapolating the best-fitting model to low fluxes and integrating to a maximum redshift of 2.5, amounts to 63 per cent of the observed background intensity. The uncertainty on this figure is difficult to quantify – it depends on $z_{max}$, $C$ and other parameters not constrained by the *Ginga* fluctuation results. While the uncertainty could, in principle, be ~20 per cent, the model would then have the wrong spectral shape at 4 keV. Smaller values of $N_{22}$ do not give enough difference between the $P(D)$ and the EMSS counts. Larger

values, or the same value extending to a higher $L_{abs}$, start to affect the predicted fluctuation spectrum significantly. In reality we expect that there are distributions of $N_{22}$, $L_{min}$ and $L_{abs}$, so that not all low-luminosity sources are affected in the same way. Without much better samples of AGN spectra to constrain so many variables, we cannot be more specific about the details at the present time. We require simply that the appropriately weighted means of these distributions influence the spectra and counts in the same manner as the results quoted above.

Note that the effects of redshift and absorption mean that the apparent luminosity evolution of sources in our model appears steeper in soft X-rays than in harder X-rays. Current estimates of the luminosity evolution of AGN based upon soft X-ray luminosity functions are overestimated if some correction for luminosity-dependent, intrinsic absorption is required and not made. This means that X-ray evolution, which without such corrections is slower than at optical wavelengths, is even slower than previously assumed. Whether there are similar corrections to be applied to reddened Seyfert 2 galaxies, for example, in the optical band, remains to be seen.

## 4   CONCLUSIONS

The main conclusions from our analysis of the spatial fluctuations in the XRB measured by *Ginga* are as follows.

1. The $\log N$–$\log S$ relation in the 2–10 keV band follows the form, $N(S)\,dS = 2 \times 10^{-15} S^{-2.5}\,dS$, down to $S \sim 5 \times 10^{-13}$ erg cm$^{-2}$ s$^{-1}$. The surface density of extragalactic X-ray sources at this flux limit is ~1 object per square degree, at which point approximately 10 per cent of the 2–10 keV XRB intensity is directly accounted for in terms of discrete sources.

2. The excess variance technique provides a tight upper limit to the inhomogeneities in the source distribution and direct evidence for the large-scale isotropy of the Universe out to redshifts $z \sim 1$.

3. The spectral properties of the XRB fluctuations are consistent with the average 2–10 keV source having a spectral slope close to the canonical AGN value. Tentative evidence for high-energy hardening is found which might be interpreted in terms of a reflection bump present in the sources that dominate the fluctuations. The softer spectra of clusters contributing to the fluctuations may partly mask the absorption in the AGN component.

4. The normalization of 2–10 keV source counts is a factor of 2–3 above that derived from the EMSS if a spectral conversion is assumed which ignores absorption effects. It is proposed that the EMSS underestimates the number of low-luminosity AGN as a result of intrinsic absorption. The revised estimate of the surface density of extragalactic sources is of particular importance when considering the confusion limit of imaging systems operating above ~2 keV. For an X-ray mission with an effective resolution of $\Omega_{eff} \sim 1$ arcmin$^2$, the confusion limit will be reached at a flux of about $10^{-14}$ erg cm$^{-2}$ s$^{-1}$.

### Postscript

The work described in this paper was completed in late 1994 but due to a number of unfortunate compounding factors its

publication has been subject to protracted delay. In the interim there have been major developments in the field stemming from the source counts measured by *ROSAT* and *ASCA*. The *ROSAT* source counts reach unprecedentedly faint levels in the soft X-ray (0.5–2 keV) band revealing a high density of sources ($> 400 \, \mathrm{deg}^{-1}$ at $S = 2 \times 10^{-15}$ erg $\mathrm{cm}^{-2} \, \mathrm{s}^{-1}$) which contribute over half of the X-ray background in this band (Hasinger et al. 1993; Branduardi-Raymont et al. 1994; Georgantopoulos et al. 1996). However, in the relevant flux range, the *ROSAT* source counts are fully consistent with the earlier EMSS results; thus our detailed comparison of the *Ginga* results with those from EMSS is still valid. In the medium energy 2–10 keV X-ray band to which our fluctuation measurements apply, estimates have recently become available of the discrete source detection rate in deep *ASCA* observations. These preliminary results from *ASCA*, albeit based on limited source statistics (e.g. Inoue et al. 1996; Georgantopoulos et al. 1997), appear to be in very good agreement with the *Ginga* measurements in terms of the normalization of the $\log N - \log S$ curve at a flux of $5 \times 10^{-13}$ erg $\mathrm{cm}^{-2} \, \mathrm{s}^{-1}$. The existence of a major X-ray source population characterized by either intrinsically flat or absorbed spectra is thus confirmed. For a review of other recent developments relating to our understanding of the wide-band X-ray to $\gamma$-ray extragalactic background, see Hasinger (1997).

## ACKNOWLEDGMENTS

## REFERENCES

Barcons X., 1992, ApJ, 396, 460
Barcons X., Fabian A. C., Rees M. J., 1991, Nat, 350, 685
Boldt E., 1988, in Tanaka Y., ed., Physics of Neutron Stars and Black Holes. Univ. Acad. Press, Tokyo, p. 333
Boyle B. J., Griffiths R. E., Shanks T., Stewart G. C., Georgantopoulos I., 1993, MNRAS, 260, 49
Branduardi-Raymont G. et al., 1994, MNRAS, 270, 947
Carrera F. J., Barcons X., Butcher J. A., Fabian A. C., Stewart G. C., Warwick R. S., Hayashida K., Kii T., 1991, MNRAS, 249, 698
Carrera F. J. et al., 1993, MNRAS, 260, 736
Condon J. J., 1974, ApJ, 188, 279
Edge A. C., Stewart G. C., 1991, MNRAS, 252, 414
Edge A. C., Stewart G. C., Fabian A. C., Arnaud K. A., 1990, MNRAS, 245, 559
Fabian A. C., 1975, MNRAS, 172, 149
Fabian A. C., Barcons X., 1992, ARA&A, 30, 429
Fabian A. C., Rees M. J., 1978, MNRAS, 185, 109
Georgantopoulos I., Stewart G. C., Shanks T., Boyle B. J., Griffiths R. E., 1996, MNRAS, 280, 276
Georgantopoulos I., Stewart G. C., Blair A. J., Shanks T., Griffiths R. E., Boyle B. J., Almaini O., Roche N., 1997, MNRAS, 291, 203
Gioia I. M., Henry J. P., Maccacaro T., Morris S. L., Stocke J. T., Wolter A., 1990a, ApJ, 356, L35
Gioia I. M., Maccacaro T., Schild R. E., Wolter A., Stocke J. T., Morris S. L., Henry J. P., 1990b, ApJS, 72, 567
Hasinger G., 1997, A&AS, 120, 607
Hasinger G., Burg R., Giacconi R., Hartner G., Schmidt M., Trumper J., Zamorani G., 1993, A&A, 275, 1
Hayashida K., 1990, PhD thesis, Univ. Tokyo
Hayashida K. et al., 1989, PASJ, 41, 373
Inoue H., Kii T., Ogasaka Y., Takahashi T., Ueda Y., 1996, in Zimmermann H. U., Trumper J., Yorke H., eds, Rontgenstrahlung from the Universe. MPE Report 263, 323
Maccacaro T., Gioia I. M., Wolter A., Zamorani G., Stocke J. T., 1988, ApJ, 326, 680
Maccacaro T., Della Ceca R., Gioia I. M., Morris S. L., Stocke J. T., Wolter A., 1991, ApJ, 374, 117
Marshall F. E., Boldt E. A., Holt S. S., Miller R. B., Mushotzky R. F., Rose L. A., Rothschild R. E., Serlemitsos P. J., 1980, ApJ, 235, 4
Mather J. C. et al., 1990, ApJ, 354, L37
Piccinotti G., Mushotzky R. F., Boldt E. A., Holt S. S., Marshall F. E., Serlemitsos P. J., Shafer R. A., 1982, ApJ, 253, 485
Pounds K. A., Nandra P., Stewart G. C., George I. M., Fabian A. C., 1990, Nat, 344, 132
Pye J. P., Warwick R. S., 1979, MNRAS, 187, 905
Reichert G. A., Mushotzky R. F., Petre R., Holt S. S., 1985, ApJ, 296, 69
Scheuer P. A. G., 1974, MNRAS, 166, 329
Schwartz D. A., 1979, Baity W. A., Petersen L. E., eds, X-ray Astronomy. Pergamon Press, New York, p. 453
Schwartz D. A., Murray S., Gursky H., 1976, ApJ, 204, 315
Shafer R. A., 1983, PhD thesis, Univ. Maryland, NASA TM 85029
Stocke J. T., Morris S. L., Gioia I. M., Maccacaro T., Schild R., Fleming T. A., Henry J. P., 1991, ApJS, 76, 813
Turner T. J., Pounds K. A., 1989, MNRAS, 240, 833
Turner M. J. L. et al., 1989, PASJ, 41, 345
Warwick R. S., Butcher J. A., 1992, in Koyama K., Tanaka Y., eds, Frontiers of X-ray astronomy. Univ. Acad. Press, Tokyo, p. 641
Warwick R. S., Pye J. P., 1978, MNRAS, 183, 169
Warwick R. S., Stewart G. C., 1989, in Hunt J., Battrick B., eds, X-Ray Astronomy, Vol. 2: AGN and the X-ray Background. ESA SP-296, Noordwijk, p. 727